Pushap Lata Sharma[*], *Mohini Kapalta*

DOUBLE DIFFUSIVE ELECTROCONVECTION IN ROTATING NANOFLUID SATURATED POROUS LAYER: DARCY BRINKMAN MODEL

DVOSTRUKA DIFUZIONA ELEKTROKONVEKCIJA U ROTIRAJUĆEM NANOFLUIDU SA POROZNOM SREDINOM: DARSI-BRINKMAN MODEL

Originalni naučni rad / Original scientific paper
Rad primljen / Paper received: 27.01.2025
https://doi.org/10.69644/ivk-2026-01-0101

Adresa autora / Author's address:
Department of Mathematics & Statistics, Himachal Pradesh University, Summer Hill, Shimla-171005, India
P.L. Sharma https://orcid.org/0000-0001-5848-9214 ;
M. Kapalta https://orcid.org/0009-0005-6371-4072
[*]email: pl_maths@yahoo.in

Keywords
- electric field
- rotation
- thermosolutal
- nanofluid
- porous medium
- Darcy-Brinkman model

Ključne reči
- električno polje
- rotacija
- termorastvorljivost
- nanofluid
- porozna sredina
- Darsi-Brinkman model

Abstract

This research explores the impact of rotation and vertical alternating current (AC) electric fields on the onset of convective instability within a rheological dielectric nanofluid layer heated from below and saturated by a Darcy porous medium. Linear stability analysis is employed, and the system's coupled differential equations are analytically solved under stress-free boundary conditions using the normal mode method. The study examines the influences of parameters such as the modified diffusivity ratio, AC electric Rayleigh number, nanofluid Lewis number, solutal and nanoparticle Rayleigh numbers, porosity, and Taylor number on stationary convection. Results indicate that an increasing nanofluid Lewis number, solutal and nanoparticle Rayleigh numbers, AC electric field, and modified diffusivity ratio accelerate the onset of stationary convection, while the increase of Taylor number and porosity delay it.

Izvod

U ovom radu istraživanja obuhvataju uticaje rotacije i vertikalnog električnog polja od naizmenične struje na pojavu nestabilne konvekcije unutar reološkog dielektričnog sloja nanofluida koji se zagreva odozdo, a koji je zasićen Darsi poroznom sredinom. Urađena je analiza linearne stabilnosti, a sistem spregnutih diferencijalnih jednačina se rešava analitički u graničnim uslovima bez napona, metodom u normalnom modu. U radu se proučavaju uticaji parametara kao što su modifikovani odnos difuzivnosti, Rejlejev broj za naizmeničnu struju, Luisov broj za nanofluid, Rejlejevi brojevi za rastvorljivost i nanočestice, poroznost, i Tejlorov broj za stacionarnu konvekciju. Rezultati pokazuju da sa porastom Luisovog broja za nanofluid, Rejlejevih brojeva za rastvorljivost, nanočestice i naizmenično električno polje, kao i modifikovani odnos difuzivnosti, ubrzavaju otpočinjanje stacionarne konvekcije, a sa porastom Tejlorovog broja i poroznosti se odlaže.

INTRODUCTION

In the multidisciplinary field of electro-thermo-hydrodynamics, a complex interplay between electric fields and thermal gradients gives rise to various phenomena in horizontal layers of dielectric liquids. Experimental studies in this area aim to improve heat transfer techniques by applying electric fields to dielectric fluids, providing an efficient, low-power, and cost-effective method for enhancing heat transfer. This approach also allows for precise control over enhancement dynamics.

Chand /1/ investigated electrothermal convection in a Brinkman porous medium saturated with nanofluid, finding that stationary convection is stabilised by both the Brinkman-Darcy number and the porosity parameter, resulting in more controlled and predictable flow. In contrast, factors such as the Lewis number, modified diffusivity ratio, AC electric field parameter, and nanoparticle Rayleigh number tend to destabilise stationary convection.

Chen et al. /2/ highlighted advancements in electrohydrodynamics (EHD), a field focused on fluid behaviour under electric fields, and its practical applications. Shivakumara et al. /3/ found that increasing the AC electric Rayleigh number enhances heat transfer efficiency and accelerates the onset of convection, while a higher pair stress parameter delays the onset of electrothermal convection. Additionally, Shivakumara et al. /4/ explored electrothermoconvection in a rotating porous layer modelled using the Brinkman approach, while Shivakumara et al. /5/ studied the effects of temperature and velocity boundary conditions in rotating dielectric fluid layers. Furthermore, Shivakumara et al. /6/ examined the initiation of Darcy-Brinkman electroconvection in porous media saturated with dielectric fluids, noting its relevance to geophysics, environmental science, and engineering.

The distinction between thermal and solutal diffusivities, which underpins thermosolutal convection phenomena, was initially demonstrated by Stern /7/. Wakif et al. /8/ conducted analytical and numerical studies on electroconvection in a dielectric nanofluid within a rotating Darcy porous medium. Their findings reveal that increasing parameters such as the Lewis number, AC electric Rayleigh-Darcy number, nanoparticle Rayleigh-Darcy number, or modified diffusivity ratio accelerate the onset of electroconvection, while raising the medium's porosity or the Taylor-Darcy number, delays it.

Bhadauria and Agarwal /9/ studied natural convection in a nanofluid-saturated rotating porous medium, observing a bottom-heavy distribution of nanoparticles with density decreasing upward through the porous layer. Chand and Rana /10/ explored the onset of thermal convection in a rotating nanofluid layer saturating a Darcy-Brinkman porous medium. Devi et al. /11/ analysed a rotating Jeffrey nanofluid within a porous medium for free-free, rigid-free, and rigid-rigid boundary conditions, finding that the Taylor number, Jeffrey parameter, and nanofluid Lewis number delay the onset of stationary convection, while the electric field and concentration Rayleigh number destabilise the system across all boundary types. Sharma et al. /12/ examined the influence of a magnetic field on rotating Jeffrey nanofluid saturated by a porous media.

Rotating fluids play a key role in numerous physical phenomena, such as airflow, deep convection chimneys, and the convective layer of the solar system. Understanding the Coriolis force provides insights into galaxy formation, ocean circulation, and Earth's rotation. Takashima /13/ was the first to study the combined effects of uniform rotation and an external electric field under an adverse temperature gradient. Yadav et al. /14/ found that increasing the Taylor number raises the critical wave number, reducing the size of convection cells, with the critical wave number solely dependent on the Taylor number and unaffected by nanofluid properties.

Buongiorno /15/ mechanistically described the impact of thermophoresis in nanofluids, showing that convective heat transfer enhancement primarily arises from reduced viscosity and thinning of the laminar sublayer. Thermosolutal convection in rotating nanofluid has garnered significant interest from numerous researchers over the past decade /16, 17, 18/. Kuznetsov and Nield /19/ investigated thermal instability in a porous medium saturated with a nanofluid, offering insights for cooling technologies, filtration systems, and energy extraction. Nield and Bejan /20/, in their book *Convection in Porous Media*, extensively covered the fluid flow and heat transfer in porous materials. Sheu /21/ studied thermal instability in a porous medium saturated with a viscoelastic nanofluid.

Knobloch /22/ investigated convection in binary fluids, demonstrating that the equations governing thermal convection driven by Soret and Dufour effects are equivalent to those for thermosolutal convection, with differences in the relationship between thermal and solutal Rayleigh numbers. Kuznetsov and Nield /23/ examined double-diffusive nanofluid convection in a saturated porous medium, finding that when Soret and Dufour parameters are negligible, non-oscillatory modes dominate if buoyancy forces act in opposite directions. Nield and Kuznetsov /24/ studied the conditions triggering double-diffusive convection in nanofluids, focusing on the interplay of temperature and concentration gradients.

Sharma and Kapalta /25/ analysed electrothermosolutal convection in a nanofluid-saturated porous medium, concluding that alternating current (AC) electric fields and porosity destabilise stationary convection. Sharma et al. /26/ explored the behaviour of electrohydrodynamic convection in a dielectric Oldroydian nanofluid layer permeating a porous medium. Sharma et al. /27/ found that AC electric fields destabilise convection for both bottom-heavy and top-heavy nanoparticle distributions, while the Taylor number stabilises the system for both scenarios. Pundir et al. /28/ studied double-diffusive convection in a rotating couple-stress nanofluid layer within a porous medium, finding that increased Rayleigh and Taylor numbers stabilise stationary convection. Rana and Agarwal /29/ showed that rotation significantly affects convection patterns in binary nanofluids, stabilising the fluid and delaying convection onset. Sharma and Gupta /30/ investigated double-diffusive convection in a rotating porous medium saturated with nanofluid, using the Darcy-Brinkman model to study the effects of thermal and solutal gradients and rotation on the convection process.

MATHEMATICAL FORMULATION

Consider an infinitely extended layer of dielectric rotating nanofluid, confined between two parallel surfaces situated at $z = 0$ and $z = d$, and subjected to a uniform rotation characterised by an angular velocity $\mathbf{\Omega}(0,0,\Omega)$ along the z-axis. This rotation is induced by heating the system from below. This configuration is further characterised by the saturation of a porous medium within the fluid matrix. In addition to the heating mechanism, the system is subjected to the influence of both a uniform AC electric field and a gravitational field denoted as $\mathbf{g} = -g\hat{e}_z$, acting vertically through the layers. The bottom surface and the top surface $z = d$ are maintained at constant temperatures T_0 and T_1, concentrations C_0 and C_1, and volumetric fractions ψ_0 and ψ_1, in respect. Figure 1 depicts a cartesian coordinate system (x,y,z), with the x-axis oriented parallel to the surface and the z-axis directed vertically upward.

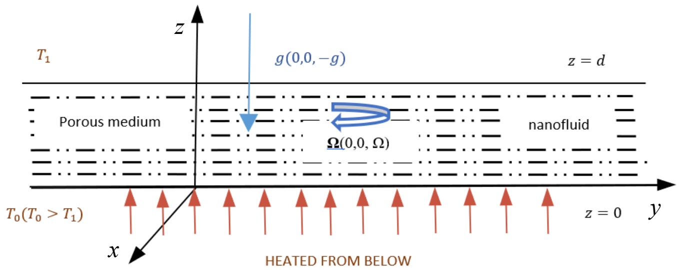

Figure 1. Physical configuration.

Governing equations

Equation of continuity for nanofluid is

$$\nabla.\mathbf{V} = 0\,, \tag{1}$$

where: $\mathbf{V}$ is nanofluid velocity.

Equations of motion for rotating dielectric Jeffrey nanofluid are

$$\frac{\rho_0}{\varepsilon}\left(\frac{\partial}{\partial t}+\frac{1}{\varepsilon}\mathbf{V}.\nabla\right)\mathbf{V} = -\nabla p + \rho\mathbf{g} + f_e - \frac{\mu}{k_1}\mathbf{V} + \mu\nabla^2\mathbf{V} + + \frac{2\rho_0}{\varepsilon}(\mathbf{V}\times\mathbf{\Omega})\,, \tag{2}$$

where: ρ_0 is reference density for the fluid; μ is viscosity; and f_e is electrical force given by

$$f_e=\rho_e\mathbf{E}-\frac{1}{2}\mathbf{E}^2\nabla\gamma+\frac{1}{2}\nabla\left(\rho\frac{\partial\gamma}{\partial t}\mathbf{E}^2\right),$$

where: ρ_e is density of charge; γ is dielectric constant; $\mathbf{E}$ is electric field. The term $\rho_e\mathbf{E}$ associated with free charge is attributed to the Coulomb force which governs the interaction between charged particles within the dielectric fluid. This force is typically the dominant effect in such systems, where the electric field exerts a direct influence on the free charges. The second term, known as the dielectrophoretic force, arises due to the force exerted on a dielectric fluid in the presence of a nonuniform electric field. This effect is typically weaker than the Coulomb force and becomes particularly relevant under alternating current (AC) electric fields. Therefore, the term $\rho_e\mathbf{E}$ is neglected as compared to the term $-\mathbf{E}^2\nabla\gamma/2$ for most dielectric fluids.

The final term, the gradient of a scalar field, typically represents the pressure gradient in fluid dynamics. While it contributes to the overall governing equations of the system, its impact on the instability of the dielectric fluid is minimal. As such, it is often assumed to have no significant effect on the instability behaviour of the fluid, especially in the context of electric field-induced phenomena.

Therefore, the modified pressure term is

$$P=p-\frac{1}{2}\left(\rho\frac{\partial\gamma}{\partial t}\mathbf{E}^2\right), \tag{3}$$

where: p is hydrodynamical pressure.

In the absence of free charge, Maxwell's equations are

$$\nabla.(\gamma\mathbf{E})=0,\quad \nabla\times\mathbf{E}=0\cdot \tag{4}$$

From Eq.(4), $\mathbf{E}$ can be shown as

$$\mathbf{E}=-\nabla\xi, \tag{5}$$

where: ξ is root mean square value of the electric potential.

The dielectric constant is considered as

$$\gamma=\gamma_0(1-\alpha(T-T_0))\cdot \tag{6}$$

Additionally, ρ represents the total density of the nanofluid, which is expressed

$$\rho=\psi\rho_p+(1-\psi)\rho_0(1-\eta_T(T-T_0)-\eta_S(C-C_0))\cdot \tag{7}$$

Here, ψ is the volumetric fraction of nanoparticles, ρ_p is the density of nanoparticles, η_T is the thermal volumetric expansion coefficient, η_S is the analogous solutal coefficient, and C is solute concentration.

Consequently, the revised momentum Eqs.(2) for concentrated nanofluid, incorporating Eq.(8) in the presence of an electric field, are expressed as

$$\frac{\rho_0}{\varepsilon}\left(\frac{\partial}{\partial t}+\frac{1}{\varepsilon}\mathbf{V}.\nabla\right)\mathbf{V}=-\nabla P-\frac{1}{2}\mathbf{E}^2\nabla\gamma-\frac{\mu}{k_1}\mathbf{V}+\frac{2\rho_0}{\varepsilon}(\mathbf{V}\times\mathbf{\Omega})+$$
$$+[\psi\rho_p+(1-\psi)\rho_0(1-\eta_T(T-T_0)-\eta_S(C-C_0))]\mathbf{g}+\mu\nabla^2\mathbf{V}\cdot \tag{8}$$

The energy equation for a nanofluid in a porous medium can be expressed as

$$(\rho C)_m\frac{\partial T}{\partial t}+(\rho C)_f(\mathbf{V}.\nabla)T=\kappa_m\nabla^2T+\varepsilon(\rho C)_p\times$$
$$\times\left(D_B\nabla\psi.\nabla T+\frac{D_T}{T}\nabla T.\nabla T\right), \tag{9}$$

where: $(\rho C)_f$ is heat capacity of fluid; $(\rho C)_p$ is heat capacity of nanoparticles; D_B is Brownian diffusion coefficient; D_T is the thermophoresis diffusion coefficient.

The governing equation for the solute in conservative form is

$$\left(\frac{\partial}{\partial t}+\frac{1}{\varepsilon}\mathbf{V}.\nabla\right)C=D_{SL}\nabla^2C, \tag{10}$$

where: D_{SL} is solutal diffusivity.

The governing equation for the nanoparticles in conservative form is

$$\left(\frac{\partial}{\partial t}+\frac{1}{\varepsilon}\mathbf{V}.\nabla\right)\psi=D_B\nabla^2\psi+\frac{D_T}{T}\nabla^2T\cdot \tag{11}$$

This implies that the nanoparticles move uniformly along with the fluid.

The conditions at the boundaries are

$$T=T_0,\ C=C_0,\ \psi=\psi_0\quad\text{at}\quad z=0,$$
$$T=T_1,\ C=C_1,\ \psi=\psi_1\quad\text{at}\quad z=d. \tag{12}$$

The system is initially in a state of rest, represented as

$$\mathbf{V}=\mathbf{V_b}=\mathbf{0},\ T=T_b(z),\ C=C_b(z),\ \psi=\psi_b(z),$$
$$P=P_b(z),\ \mathbf{E}=\mathbf{E_b}(z),\ \gamma=\gamma_b(z)\cdot \tag{13}$$

By using Eq.(13) into Eqs.(1), (4)-(6) and (8)-(11), we get

$$T_b=T_0-\frac{\Delta T}{d}z,\ \psi_b=\psi_0-\frac{\psi_1-\psi_0}{d}z,$$
$$\gamma_b=\gamma_0\left(1+\alpha\frac{\Delta T}{d}z\right),\ E_b(z)=\frac{E_0}{1+\alpha\frac{\Delta T}{d}z},$$
$$C_b=C_0-\frac{\Delta C}{d}z,\ \xi_b=-\frac{E_0h}{\alpha\Delta T}\ln\left(1+\alpha\frac{\Delta T}{d}z\right), \tag{14}$$

where: $E_0=-\alpha\Delta T\xi_1/d\ln(1+\alpha\Delta T)$ represents the root mean square value of the electric field at $z=d$.

Perturbed state

To analyse the stability of the basic state, we introduce infinitesimally small perturbations to the basic state in the following form

$$\mathbf{V}=\mathbf{V}'(u',v',w'),\ P=P_b+P',\ T=T_b+T',\ C=C_b+C',$$
$$\psi=\psi_b+\psi',\ E=E_b+E',\ \xi=\xi_b+\xi',\ \gamma=\gamma_b+\gamma'\cdot \tag{15}$$

By substituting the values from Eq.(15) into Eqs.(1), (4)-(11), utilising Eq.(14), and linearising the equations while disregarding the products of primed quantities, we eliminate the pressure from the momentum equation through a double curl operation. By retaining only, the vertical component and omitting the primes (′) for simplicity, the resulting necessary equations are obtained as follows

$$\left(\frac{1}{\varepsilon}\frac{\partial}{\partial t}+\frac{\nu}{k_1}-\nu\nabla^2\right)\nabla^2w=-\frac{\alpha\gamma_0\Delta TE_0}{\rho_0}\nabla_H^2\left(\alpha E_0T-\frac{\partial\xi}{\partial z}\right)-$$
$$-\frac{2}{\varepsilon}\Omega\frac{\partial\zeta}{\partial z}+\nabla_H^2\left[-\psi\left(\frac{\rho_p-\rho_0}{\rho_0}\right)+(\eta_TT+\eta_SC)\right]g, \tag{16}$$

$$\frac{1}{\varepsilon}\frac{\partial\zeta}{\partial t}=\frac{2}{\varepsilon}\Omega\frac{\partial w}{\partial z}-\frac{\nu}{k_1}\zeta-\nu\nabla^2\zeta, \tag{17}$$

$$(\rho C)_m\frac{\partial T}{\partial t}-(\rho C)_f\frac{\Delta T}{h}w=-\frac{(\rho C)_p}{d}\frac{2\Delta TD_T}{T_1}\frac{\partial T}{\partial z}\kappa_m\nabla^2T+$$
$$+(\rho C)_pD_B\left(\frac{\psi_1-\psi_0}{d}\frac{\partial T}{\partial z}-\frac{\Delta T}{d}\frac{\partial\psi}{\partial z}\right), \tag{18}$$

$$\frac{\partial C}{\partial t}-\frac{\Delta C}{d}\frac{w}{\varepsilon}=D_{SL}\nabla^2C, \tag{19}$$

$$\frac{\partial\psi}{\partial t}+\frac{\psi_1-\psi_0}{d}\frac{w}{\varepsilon}=D_B\nabla^2\psi+\frac{D_T}{T_1}\nabla^2T, \tag{20}$$

$$\nabla^2\xi=\alpha E_0\frac{\partial T}{\partial z}\,, \tag{21}$$

where: $\zeta=\frac{\partial v}{\partial x}-\frac{\partial u}{\partial y}$ is z-component of vorticity; $\nabla^2=\frac{\partial^2}{\partial x^2}+\frac{\partial^2}{\partial y^2}+\frac{\partial^2}{\partial z^2}$ donates the three-dimensional Laplacian operator, while $\nabla_H^2=\frac{\partial^2}{\partial x^2}+\frac{\partial^2}{\partial y^2}$ represents the two-dimensional Laplacian operator.

Further, eliminating ζ from Eqs.(16) and (17), we get

$$\left(\frac{1}{\varepsilon}\frac{\partial}{\partial t}+\frac{\nu}{k_1}-\nu\nabla^2\right)^2\nabla^2 w=-\frac{4}{\varepsilon^2}\Omega^2\frac{\partial^2 w}{\partial z^2}+\left(\frac{1}{\varepsilon}\frac{\partial}{\partial t}+\frac{\nu}{k_1}-\nu\nabla^2\right)\left[-\frac{\alpha\gamma_0\Delta T E_0}{\rho_0}\nabla_H^2\left(\alpha E_0 T-\frac{\partial\xi}{\partial z}\right)\right]+\left(\frac{1}{\varepsilon}\frac{\partial}{\partial t}+\frac{\nu}{k_1}-\nu\nabla^2\right)\times$$
$$\times\left[\nabla_H^2\left(-\psi\left(\frac{\rho_p-\rho_0}{\rho_0}\right)+(\eta_T T+\eta_S C)\right)g\right]. \tag{22}$$

Non-dimensionalisation

The non-dimensional parameters are considered as

$$(x^*,y^*,z^*)=\frac{(x,y,z)}{d},\ (u^*,v^*,w^*)=d\frac{(u,v,w)}{\beta},\ T^*=\frac{T-T_0}{\Delta T},\ C^*=\frac{C-C_0}{\Delta C},\ \psi^*=\frac{\psi-\psi_0}{\psi_1-\psi_0},\ t^*=\frac{t\beta}{\sigma d^2},\ \xi^*=\frac{\xi}{\alpha E_0\Delta T d}, \tag{23}$$

where: $\beta=\kappa_m/(\rho C)_f$; and $\sigma=(\rho C)_m/(\rho C)_f$.

Using parameters Eq.(23) in Eqs.(18)-(22), dropping the star (*) for simplification), we get

$$\left(\frac{1}{\sigma V_a}\frac{\partial}{\partial t}-D_a\nabla^2+1\right)^2\nabla^2 w=-T_a\frac{\partial^2 w}{\partial z^2}+\left(\frac{1}{\sigma V_a}\frac{\partial}{\partial t}-D_a\nabla^2+1\right)\left[R_a\nabla_H^2 T-R_n\nabla_H^2\psi+\frac{R_s}{L_e}\nabla_H^2 C+R_{ef}\nabla_H^2\left(T-\frac{\partial\xi}{\partial z}\right)\right], \tag{24}$$

$$\frac{\partial T}{\partial t}-w=\nabla^2 T+\frac{N_B}{L_n}\left(\frac{\partial T}{\partial z}-\frac{\partial\psi}{\partial z}\right)-\frac{2N_A N_B}{L_n}\frac{\partial T}{\partial z}, \tag{25}$$

$$\frac{1}{\sigma}\frac{\partial C}{\partial t}-\frac{w}{\varepsilon}=\frac{1}{L_e}\nabla^2 C\,, \tag{26}$$

$$\frac{1}{\sigma}\frac{\partial\psi}{\partial t}+\frac{w}{\varepsilon}=\frac{1}{L_n}\nabla^2\psi+\frac{N_A}{L_n}\nabla^2 T\,, \tag{27}$$

$$\nabla^2\xi=\frac{\partial T}{\partial z}\,, \tag{28}$$

where: the non-dimensional parameters are $V_a=\varepsilon P_r/D_a$ is Vadasz number; $D_a=k_1/d^2$ is Darcy number; $P_r=\nu/\beta$ is Prandtl number; $R_a=\eta_T\Delta T k_1 dg/\beta\nu$ is the thermal Rayleigh number; $R_n=(\rho_p-\rho_0)(\psi_1-\psi_0)k_1 dg/\beta\mu$ is the nanoparticle Rayleigh number; $R_s=\eta_S\Delta C k_1 dg/\beta\nu$ is the solutal Rayleigh number; $R_{ef}=\zeta_0\alpha^2(\Delta T)^2E_0^2k_1 d/\beta\mu$ is the AC electric field Rayleigh number; $L_n=\beta/D_B$ is nanofluid Lewis number; $L_e=\beta/D_{ST}$ is solutal Lewis number; $T_a=(2\Omega k_1/\varepsilon\nu)^2$ is the Taylor number; $N_A=D_T\Delta T/D_B T_1(\psi_1-\psi_0)$ is the modified diffusivity ratio; $N_B=[(\rho C)_p/(\rho C)_f](\psi_1-\psi_0)$ is modified particle-density increment.

The boundary conditions Eq.(12), for free boundaries is given by

$$T=C=w=\psi=0\quad\text{at}\quad z=0\quad\text{and}\quad z=1,$$
$$\frac{\partial^2 w}{\partial z^2}=0,\quad\frac{\partial\xi}{\partial z}=0\quad\text{for free surfaces.} \tag{32}$$

Linear stability analysis

For linear stability analysis, we employ the normal mode method, which assumes solutions of the form

$$(w,T,C,\psi,\xi)=(W,\Theta,\Phi,\Psi,\Upsilon)(z)\exp(i(px+qy)+st)\,, \tag{30}$$

where: p and q represent horizontal wave numbers; and s denotes the growth rate, which is a complex value.

By substituting Eq.(30) into Eqs.(24)-(28), we obtain

$$\left(\frac{s}{\sigma V_a}-D_a(D^2-a^2)+1\right)\left(a^2(R_a+R_{ef})\Theta-a^2R_n\Psi+a^2\frac{R_s}{L_e}\Phi-a^2R_{ef}D\Upsilon\right)+\left[\left(\frac{s}{\sigma V_a}-D_a(D^2-a^2)+1\right)^2(D^2-a^2)+T_aD^2\right]W=0, \tag{31}$$

$$W+\left((D^2-a^2)+\frac{N_B}{L_n}D-\frac{2N_AN_B}{L_n}D-s\right)\Theta-\frac{N_B}{L_n}D\Psi=0, \tag{32}$$

$$\frac{W}{\varepsilon}+\left(\frac{1}{L_e}(D^2-a^2)-\frac{s}{\sigma}\right)\Phi=0, \tag{33}$$

$$\frac{W}{\varepsilon}-\frac{N_A}{L_n}(D^2-a^2)\Theta+\left(\frac{s}{\sigma}-\frac{1}{L_n}(D^2-a^2)\right)\Psi=0, \tag{34}$$

$$D\Theta-(D^2-a^2)\Upsilon=0, \tag{35}$$

where: $D=d/dz$; and $a=\sqrt{(p^2+q^2)}$ is wave number.

NUMERICAL SOLUTION

After applying the normal mode analysis, the boundary conditions Eq.(29) become

$$W=D^2W=\Theta=\Phi=\Psi=D\Upsilon=0\quad\text{at}\quad z=0,1\,. \tag{36}$$

The simplest functions of lowest mode that satisfy the boundary conditions Eq.(36) are assumed to be

$$W=A_1\sin\pi z,\quad\Theta=A_2\sin\pi z,\quad\Phi=A_3\sin\pi z,$$
$$\Psi=A_4\sin\pi z,\quad\Upsilon=A_5\cos\pi z. \tag{37}$$

By substituting Eq.(37) into Eqs.(31)-(35), we obtain a system of homogeneous linear equations, which has a non-trivial solution only if the determinant of the corresponding coefficients matrix is zero i.e.,

$$\begin{vmatrix} (J'^2 J+\pi^2 T_a) & -a^2(R_a+R_{ef})J' & -a^2\dfrac{R_s}{L_e}J' & a^2 R_n J' & -\pi a^2 R_{ef} J' \\ -1 & J+s & 0 & 0 & 0 \\ -\dfrac{1}{\varepsilon} & 0 & \dfrac{1}{L_e}J+\dfrac{s}{\sigma} & 0 & 0 \\ \dfrac{1}{\varepsilon} & \dfrac{N_A}{L_n}J & 0 & \dfrac{1}{L_n}J+\dfrac{s}{\sigma} & 0 \\ 0 & \pi & 0 & 0 & J \end{vmatrix}=0, \tag{38}$$

where: $J'=\dfrac{s}{\sigma V_a}+D_a(\pi^2+a^2)+1$; and $J=\pi^2+a^2$.

On solving Eq.(38), we get the following thermal Rayleigh number

$$R_a=(\pi^2+a^2)\left(\frac{\pi^2+a^2+s}{a^2}\right)\left(\frac{s}{\sigma V_a}+D_a(\pi^2+a^2)+1\right)-\frac{a^2R_{ef}}{\pi^2+a^2}-\frac{R_s(\pi^2+a^2+s)}{\varepsilon\left(\pi^2+a^2+\frac{s}{\sigma}L_e\right)}+\frac{(\pi^2+a^2)(\pi^2+a^2+s)T_a}{a^2\left(\frac{s}{\sigma V_a}+D_a(\pi^2+a^2)+1\right)}+$$
$$+\frac{R_n}{\pi^2+a^2+\frac{s}{\sigma}L_n}\left(\frac{s}{\varepsilon}L_n+(\pi^2+a^2)\left(N_A+\frac{L_n}{\varepsilon}\right)\right). \tag{39}$$

Equation (39) represents the dispersion relation which incorporates the effect of electric field Rayleigh number R_{ef}, Vadasz number V_a, the nanofluid Lewis number L_n, solutal Lewis number L_e, solutal Rayleigh number R_S, modified diffusivity ratio N_A, nanoparticle Rayleigh number R_n and Darcy number D_a.

Stationary convection

In the case of stationary convection, by substituting $s = 0$ in Eq.(39), we get

$$R_a=\frac{(\pi^2+a^2)}{a^2}(D_a(\pi^2+a^2)+1)-\frac{a^2R_{ef}}{\pi^2+a^2}-\frac{R_s}{\varepsilon}+$$
$$+\frac{\pi^2(\pi^2+a^2)T_a}{a^2(D_a(\pi^2+a^2)+1)}-R_n\left(N_A+\frac{L_n}{\varepsilon}\right). \tag{40}$$

The thermal Rayleigh number depends on Darcy number D_a, AC electric Rayleigh number R_{ef}, nanofluid Lewis number L_n modified diffusivity ratio N_A, Taylor number T_a, solutal Rayleigh number R_S, porosity ε, and the nanoparticle Rayleigh number R_n.

Without R_{ef} and R_S the Eq.(40) simplifies to

$$R_a=\frac{(\pi^2+a^2)}{a^2}(D_a(\pi^2+a^2)+1)+\frac{\pi^2(\pi^2+a^2)T_a}{a^2(D_a(\pi^2+a^2)+1)}-$$
$$-R_n\left(N_A+\frac{L_n}{\varepsilon}\right), \tag{41}$$

which makes good agreement with the result proved by Bhadauria and Agarwal /9/.

Further for $T_a = 0$, Eq.(41) reduces to

$$R_a=\frac{(\pi^2+a^2)}{a^2}(D_a(\pi^2+a^2)+1)-R_n\left(N_A+\frac{L_n}{\varepsilon}\right), \tag{42}$$

which is consistent with the findings established by Kuznetsov and Nield /19/.

Further for $D_a = 0$, we obtain

$$R_a=\frac{(\pi^2+a^2)}{a^2}-R_n\left(N_A+\frac{L_n}{\varepsilon}\right), \tag{43}$$

which is consistent with the findings established by Sheu /21/.

The critical value of R_a is determined by differentiating Eq.(40) w.r.t. a^2 and set to zero, we get

$$A_1(a_c^2)^7+A_2(a_c^2)^6+A_3(a_c^2)^5+A_4(a_c^2)^4+A_5(a_c^2)^3+$$
$$+A_6(a_c^2)^2+A_7(a_c^2)+A_8=0, \tag{44}$$

where:
$$A_1=2D_a^3, \tag{45}$$
$$A_2=11\pi^2D_a^3+5D_a^2, \tag{46}$$
$$A_3=24\pi^4D_a^3+22\pi^2D_a^2+4D_a, \tag{47}$$
$$A_4=25\pi^6D_a^3+(35\pi^4-\pi^2R_{ef})D_a^2+1+(13\pi^2-\pi^2T_a)D_a, \tag{48}$$
$$A_5=10\pi^8D_a^3+(20\pi^6-2\pi^4R_{ef})D_a^2+2\pi^2+(12\pi^4-$$
$$-2\pi^2R_{ef}-4\pi^4T_a)D_a, \tag{49}$$
$$A_6=-3\pi^{10}D_a^3-(5\pi^8+\pi^6R_{ef})D_a^2-\pi^2R_{ef}-\pi^4T_a-$$
$$-(2\pi^6+2\pi^4R_{ef}+6\pi^6T_a)D_a, \tag{50}$$
$$A_7=-4\pi^{12}D_a^3-10\pi^{10}D_a^2-2\pi^6-2\pi^6T_a+(-8\pi^8-4\pi^8T_a)D_a, \tag{51}$$
$$A_8=-\pi^{14}D_a^3-3\pi^{12}D_a^2-\pi^8-\pi^8T_a+(-3\pi^{10}-\pi^{10}T_a)D_a. \tag{52}$$

These equations are solved for various values of AC electric Rayleigh number, yielding the corresponding values of a_c.

To analyse the effects of the AC electric field, the Taylor number, concentration Rayleigh number, solutal Rayleigh number, porosity, Darcy number, modified diffusivity ratio, and nanofluid Lewis number, on stationary convection, we examine the analytical behaviour of the partial derivatives: $\partial R_a/\partial R_{ef}$, $\partial R_a/\partial T_a$, $\partial R_a/\partial R_n$, $\partial R_a/\partial R_S$, $\partial R_a/\partial\varepsilon$, $\partial R_a/\partial D_a$, $\partial R_a/\partial N_a$, and $\partial R_a/\partial L_n$.

From Eq.(40), we obtain

$$\frac{\partial R_a}{\partial R_{ef}}=-\frac{a^2}{\pi^2+a^2}. \tag{53}$$

This value is consistently negative for all wave numbers, indicating that the AC electric field exerts a destabilising effect on the system,

$$\frac{\partial R_a}{\partial T_a}=\frac{\pi^2(\pi^2+a^2)}{a^2[D_a(\pi^2+a^2)+1]}, \tag{54}$$

which is always positive. Hence, Taylor number delays the stationary convection,

$$\frac{\partial R_a}{\partial R_n} = -\left(N_A + \frac{L_n}{\varepsilon}\right), \tag{55}$$

which is always negative for $\left(N_A + \frac{L_n}{\varepsilon}\right) > 0$, since the value of N_A is considered in the range of 1 to 25, and L_n in the range of 500 to 1500, R_n exhibits a destabilising effect on the onset of stationary convection.

$$\frac{\partial R_a}{\partial R_S} = -\frac{1}{\varepsilon}, \tag{56}$$

which is always negative. Therefore, R_S accelerates the system,

$$\frac{\partial R_a}{\partial \varepsilon} = \frac{R_n L_n + R_S}{\varepsilon^2}, \tag{57}$$

which is positive for R_n, L_n, $R_S > 0$, hence porosity stabilises the system,

$$\frac{\partial R_a}{\partial D_a} = \frac{(\pi^2 + a^2)^3}{a^2} - \frac{\pi^2(\pi^2 + a^2)^2 T_a}{a^2[D_a(\pi^2 + a^2) + 1]^2}. \tag{58}$$

Therefore, the Darcy number delays the system for $(\pi^2 + a^2) > \pi^2 T_a/[D_a(\pi^2 + a^2) + 1]^2$ and accelerates the system for $(\pi^2 + a^2) < \pi^2 T_a/[D_a(\pi^2 + a^2) + 1]^2$,

$$\frac{\partial R_a}{\partial N_A} = -R_n, \quad \frac{\partial R_a}{\partial L_n} = -\frac{R_n}{\varepsilon}. \tag{59}$$

It is evident from Eq.(59), for positive value of R_n, the modified diffusivity ratio N_A, and nanofluid Lewis number L_n are both observed to have negative values, hence they destabilise the system for negative value of R_n.

NUMERICAL DISCUSSION

Analytical investigation of free-free boundaries reveals that oscillatory convection is not a favourable mode of instability in the context under study. Furthermore, the formulation of thermal Rayleigh number characterising stationary convection is explicated in Eqs.(40) for free-free boundaries. Subsequently, the Rayleigh number's variation relative to wave-number is graphically depicted utilising Eq.(40) and computational software, such as MATHEMATICA®, under stationary convection. The dimensional parameters are held fixed at predetermined values to ensure the integrity of the analysis, as: $T_a = 600$; $R_{ef} = 100$; $N_A = 5$; $L_n = 500$; $\varepsilon = 0.4$; $D_a = 0.5$; $R_n = 0.1$; and $R_S = 50$.

For five distinct values of AC electric Rayleigh number R_{ef} and various fixed parameters under free-free boundary conditions, Fig. 2 depicts the variation of thermal Rayleigh number for stationary convection as a function of the non-dimensional wave number. The graphs reveal that thermal Rayleigh number for stationary convection decreases with increasing values of R_{ef}. Consequently, the AC electric Rayleigh number destabilises stationary convection, effectively advancing its onset.

Figure 3 depicts the relationship between thermal Rayleigh number R_a and the wave number a for five different values of the Taylor number T_a = 0, 200, 400, 600, 1000. The results clearly demonstrate that an increase in the Taylor number leads to an increase in the thermal Rayleigh number, indicating that the Taylor number has a stabilising effect on stationary convection. Therefore, the Taylor number delays the onset of convection.

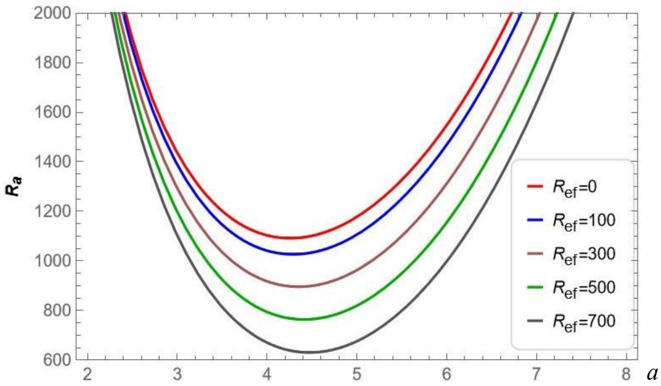

Figure 2. Variations of thermal Rayleigh number vs. non-dimensional wave number for 5 values of AC electric Rayleigh number.

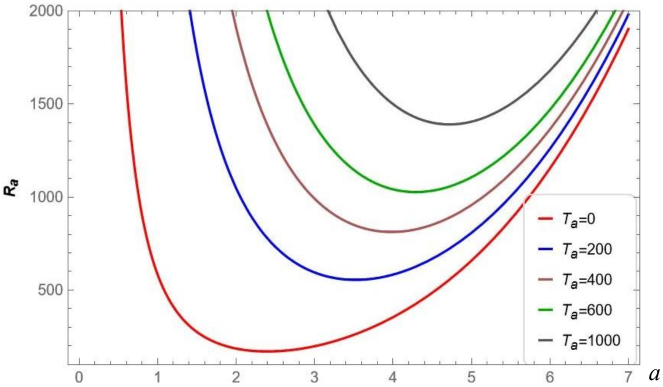

Figure 3. Variations of thermal Rayleigh number with respect to non-dimensional wave number for 5 values of Taylor number.

Figure 4 illustrates the variation of the thermal Rayleigh number R_a with respect to wave number a for different values of nanoparticle Rayleigh number R_n = 0.1, 0.5, 1, while other parameters are held constant: $T_a = 600$; $R_{ef} = 100$; $N_A = 5$; $L_n = 500$; $\varepsilon = 0.4$; $D_a = 0.5$; and $R_S = 50$. The figure clearly demonstrates that as R_n increases, the thermal Rayleigh number R_a also decreases, indicating a destabilising effect of R_n on the system. Additionally, it is evident that R_n exerts a more pronounced destabilising influence under free-free boundary conditions. Therefore, R_n significantly facilitates the onset of convection within the system.

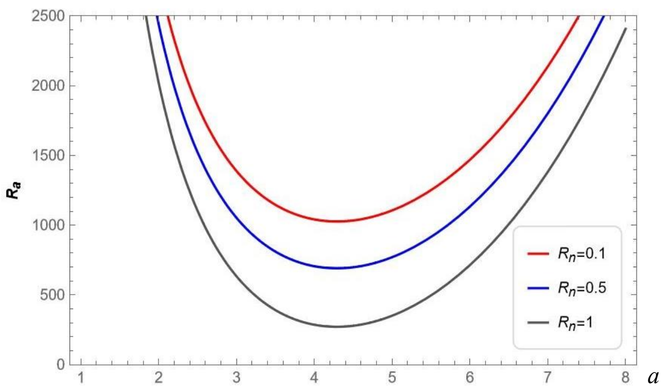

Figure 4. Changes in thermal Rayleigh number vs. dimensionless wave number for 5 values of nanoparticle Rayleigh number.

Figure 5 shows the variation of thermal Rayleigh number for stationary convection as a function of non-dimensional wave number for five distinct values of the solutal Rayleigh number R_S, with other parameters held constant at fixed permissible values. As the value of R_S increases, the thermal Rayleigh number decreases, leading to a destabilising effect on stationary convection.

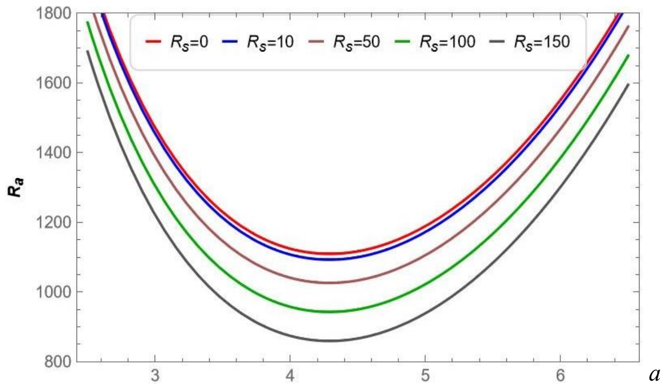

Figure 5. Variations of R_a with respect to dimensionless wave number for 5 different values of R_S.

Figure 6 illustrates the effect of medium porosity ε on thermal Rayleigh number. It is observed that as the medium porosity increases, the stationary thermal Rayleigh number also increases. Therefore, medium porosity has a stabilising effect on the system in the case of stationary convection. Therefore, ε significantly delays the onset of convection within the system.

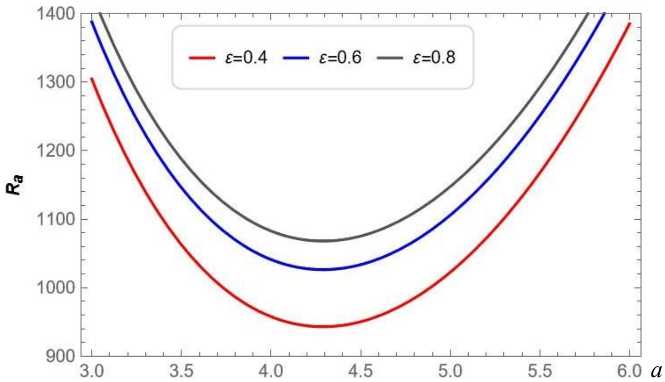

Figure 6. Variations in Rayleigh number as a function of dimensionless wave number for 3 different values of porosity.

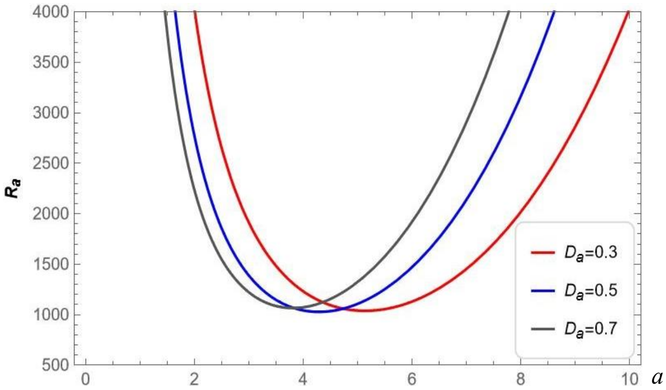

Figure 7. Variations of Rayleigh number as a function of dimensionless wave number for 3 distinct values of Darcy number.

Figure 7 presents the effect of Darcy number D_a on the neutral curves. The graphs reveal that the thermal Rayleigh number initially decreases as the Darcy number increases; however, beyond certain values of the wave number, thermal Rayleigh number begins to rise. Thus, the Darcy number exhibits a dual effect both stabilising and destabilising, due to the presence of rotation in stationary convection.

Figure 8 depicts the variation of Rayleigh number for stationary convection as a function of the dimensionless wave number for three distinct values of modified diffusivity ratio N_A, with other parameters held at fixed suitable values. The plots reveal that as modified diffusivity ratio increases, the thermal Rayleigh number decreases. Hence, the modified diffusivity ratio has a destabilising effect on the physical system.

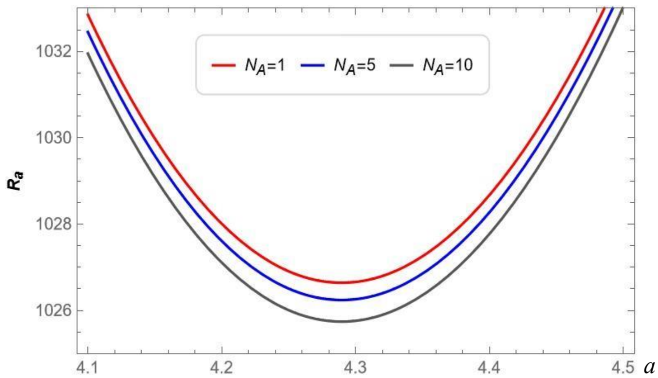

Figure 8. Variations in Rayleigh number with respect to the dimensionless wave number for 3 different values of N_A.

Figure 9 depicts the changes in Rayleigh number R_a as a function of dimensionless wave number for five different values of nanofluid Lewis number L_n = 100, 500, 1000, 1500, 2000, while other parameters are fixed as: T_a = 600; R_{ef} = 100; N_A = 5; ε = 0.4; D_a = 0.5; R_n = 0.1; and R_S = 50. The figure demonstrates that R_a decreases with an increase in L_n, indicating that nanofluid Lewis number has a destabilising effect on the onset of convection. Thus, L_n effectively accelerates the onset of convection in the system.

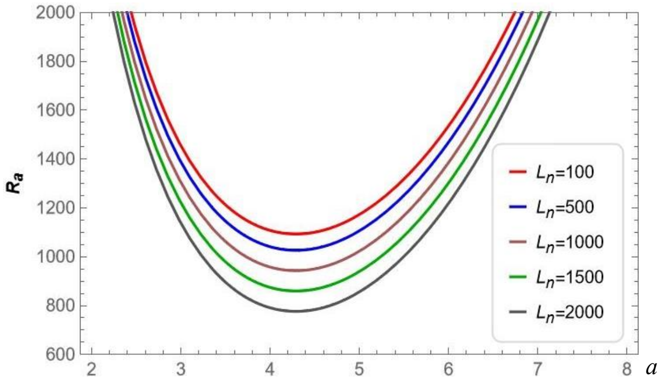

Figure 9. Variations in Rayleigh number as a function of dimensionless wave number for 5 values of nanofluid Lewis number.

CONCLUSIONS

The study investigates the onset of thermosolutal convection in an electrically conducting rheological nanofluid saturated within a porous medium, incorporating the effects of an external vertical AC electric field using linear stability theory. The main conclusions derived from this analysis are outlined below.

The nanofluid Lewis number L_n, tends to promote the destabilisation of stationary convection.

The Taylor number and medium porosity have a stabilising effect on stationary convection.

The presence of an AC electric field accelerates stationary convection.

The Darcy number stabilises the system for stationary convection at $(\pi^2 + a^2) > \pi^2 T_a / [D_a(\pi^2 + a^2) + 1]^2$ but exhibits a destabilising effect at $(\pi^2 + a^2) < \pi^2 T_a / [D_a(\pi^2 + a^2) + 1]^2$, showcasing its dual influence on the system.

The modified diffusivity ratio N_A also contributes to the destabilisation of stationary convection.

Both, the nanoparticles Rayleigh number R_n and solutal Rayleigh number R_S contribute to the destabilisation of stationary convection.

REFERENCES

1. Chand, R. (2017), *Electro-thermal convection in a Brinkman porous medium saturated by nanofluid*, Ain Shams Eng. J, 8 (4): 633-641. doi: 10.1016/j.asej.2015.10.008
2. Chen, X., Cheng, J., Yin, X. (2003), *Advances and applications of electrohydrodynamics*, Chinese Sci. Bull. 48: 1055-1063. doi: 10.1007/BF03185753
3. Shivakumara, I.S., Akkanagamma, M., Ng, C.-O. (2013), *Electrohydrodynamic instability of a rotating couple stress dielectric fluid layer*, Int. J Heat Mass Transf. 62: 761-771. doi: 10.1016/j.ijheatmasstransfer.2013.03.050
4. Shivakumara, I.S., Ng, C.-O., Nagashree, M.S. (2011), *The onset of electrothermoconvection in a rotating Brinkman porous layer*, Int. J Eng. Sci. 49(7): 646-663. doi: 10.1016/j.ijengsci.2011.02.010
5. Shivakumara, I.S., Lee, J., Vajravelu, K., Akkanagamma, M. (2012), *Electrothermal convection in a rotating dielectric fluid layer: Effect of velocity and temperature boundary conditions*, Int. J Heat Mass Transf. 55(11-12): 2984-2991. doi: 10.1016/j.ijheatmasstransfer.2012.02.010
6. Shivakumara, I.S., Rudraiah, N., Lee, J., Hemalatha, K. (2011), *The onset of Darcy-Brinkman electroconvection in a dielectric fluid saturated porous layer*, Transp. Porous Med. 90: 509-528. doi: 10.1007/s11242-011-9797-7
7. Stern, M.E. (1960), *The 'salt-fountain' and thermohaline convection*, Tellus, 12(2): 172-175. doi: 10.1111/j.2153-3490.1960.tb01295.x
8. Wakif, A., Boulahia, Z., Sehaqui, R. (2016), *Analytical and numerical study of the onset of electroconvection in a dielectric nanofluid saturated a rotating Darcy porous medium*, Int. J Adv. Comp. Sci. Appl. 7(8): 299-311. doi: 10.14569/IJACSA.2016.070841
9. Bhadauria, B.S., Agarwal, S. (2011), *Natural convection in a nanofluid saturated rotating porous layer: A nonlinear study*, Transp. Porous Med. 87: 585-602. doi: 10.1007/s11242-010-9702-9
10. Chand, R., Rana, G.C. (2012), *On the onset of thermal convection in rotating nanofluid layer saturating a Darcy-Brinkman porous medium*, Int. J Heat Mass Transf. 55(21-22): 5417-5424. doi: 10.1016/j.ijheatmasstransfer.2012.04.043
11. Devi, J., Sharma, V., Kapalta, M. (2023), *Electroconvection in rotating Jeffrey nanofluid saturating porous medium: free-free, rigid- free, rigid-rigid boundaries*, J Nanofluids, 12(6): 1554-1565. doi: 10.1166/jon.2023.2039
12. Sharma, P.L., Kumar, A., Rana, G.C. (2024), *Effect of magnetic field on thermal instability in rotating Jeffrey nanofluid saturated by a porous medium: free-free, rigid-rigid and rigid-free boundary conditions*, Struct. Integr. Life, 24(3): 315-322. doi: 10.69644/ivk-2024-03-0315
13. Takashima, M. (1976), *The effect of rotation on electrohydrodynamic instability*, Can. J Phy. 54(3): 342-347. doi: 10.1139/p76-039
14. Yadav, D., Bhargava, R., Agrawal, G.S. (2013), *Numerical solution of a thermal instability problem in a rotating nanofluid layer*, Int. J Heat Mass Transf. 63: 313-322. doi: 10.1016/j.ijheatmasstransfer.2013.04.003
15. Buongiorno, J. (2006), *Convective transport in nanofluids*, ASME J Heat Mass Transfer, 128(3): 240-250. doi: 10.1115/1.2150834
16. Sharma, P.L., Bains, D., Kumar, A., Thakur, P. (2023), *Effect of rotation on thermosolutal convection in Jeffrey nanofluid with porous medium*, Struct. Integr. Life, 23(3): 299-306.
17. Sharma, P.L., Deepak, Kumar, A. (2022), *Effects of rotation and magnetic field on thermosolutal convection in elastico-viscous Walters' (model B') nanofluid with porous medium*, Stoch. Model. Appl. 26(3): 21-30.
18. Sharma, P.L., Kumar, A., Kapalta, M., Bains, D. (2023), *Effect of magnetic field on thermosolutal convection in a rotating non-Newtonian nanofluid with porous medium*, Int. J Appl. Math. Stat. Sci. 12(1): 19-30.
19. Kuznetsov, A.V., Nield, D.A. (2010), *Thermal instability in a porous medium layer saturated by a nanofluid: Brinkman model*, Trans. Porous Media, 81(3): 409-422. doi: 10.1007/s11242-009-9413-2
20. Nield, D.A., Bejan, A., Convection in Porous Media, 5th Ed., Springer Int. Publ. AG, 2017. doi: 10.1007/978-3-319-49562-0
21. Sheu, L.J. (2011), *Thermal instability in a porous medium layer saturated with a viscoelastic nanofluid*, Transp. Porous Med. 88: 461-477. doi: 10.1007/s11242-011-9749-2
22. Knobloch, E. (1980), *Convection in binary fluids*, Phys. Fluids, 23(9): 1918-1920. doi: 10.1063/1.863220
23. Kuznetsov, A.V., Nield, D.A. (2010), *The onset of double-diffusive nanofluid convection in a layer of a saturated porous medium*, Transp. Porous Med. 85: 941-951. doi: 10.1007/s11242-010-9600-1
24. Nield, D.A., Kuznetsov, A.V. (2011), *The onset of double-diffusive convection in a nanofluid layer*, Int. J Heat Fluid Flow, 32: 771-776. doi: 10.1016/j.ijheatfluidflow.2011.03.010
25. Sharma, P.L., Kapalta, M. (2024), *Electrothermosolutal convection in nanofluid saturating porous medium*, Spec. Topics Rev. Porous Med.: An Int. J, 15(5): 41-57. doi: 10.1615/SpecialTopicsRevPorousMedia.2023049041
26. Sharma, P.L., Kapalta, M., Bains, D., et al. (2024), *Electrohydrodynamics convection in dielectric Oldroydian nanofluid layer in porous medium*, Struct. Integr. Life, 24(1): 40-48.
27. Sharma, P.L., Kapalta, M., Kumar, A., et al. (2023), *Electrohydrodynamics convection in dielectric rotating Oldroydian nanofluid in porous medium*, J Niger. Soc. Phys. Sci. 5(2): 1231(1-8). doi: 10.46481/jnsps.2023.1231
28. Pundir, S.K., Kumar, R., Pundir, R. (2022), *Double diffusive convection in a layer of saturated rotating couple-stress nanofluid in porous medium*, Int. J Sci. Res. 11(5): 1866-1872. doi: 10.21275/SR22526125759
29. Rana, P., Agarwal, S. (2015), *Convection in a binary nanofluid saturated rotating porous layer*, J Nanofluids, 4(1): 59-65. doi: 10.1166/jon.2015.1123
30. Sharma, J., Gupta, U. (2015), *Double-diffusive nanofluid convection in porous medium with rotation: Darcy-Brinkman model*, Procedia Eng. 127: 783-790. doi: 10.1016/j.proeng.2015.11.413